Diagnostic analysis of mesoscale rainstorms in the Jiang-Huai valley of China with convective vorticity vector*

Cui Xiaopeng[1**], Gao Shouting[1] and Li Xiaofan[2]

(1. Laboratory of Cloud-Precipitation Physics and Severe Storms (LACS), Institute of Atmospheric Physics, Chinese Academy of Sciences, Beijing 100029, China; 2. Joint Center for Satellite Data Assimilation and NOAA/NESDIS/Center for Satellite Applications and Research, Camp Springs, Maryland, USA)

Accepted on October 18, 2006

Abstract By the vector product of absolute vorticity vectors and equivalent potential temperature gradients, a new vector, convective vorticity vector (CVV) is readdressed after Gao et al., and is applied to the study of the development and movement of mesoscale rainstorms in the Jiang-Huai valley of China by using high-resolution simulation data with PSU/NCAR MM5 briefly. The results show that the CVV, especially its vertical component which is closely related to interactions between vertical secondary circulations and horizontal equivalent potential temperature gradients, may be a good tracer and diagnostic tool in the study of mesoscale rainstorms in the Jiang-Huai valley of China. And the main physical processes responsible for the variations of the vertical component of the CVV are discussed briefly based on its tendency equation proposed in this article.

Keywords: convective vorticity vector, mesoscale rainstorms, tendency equations.

Potential vorticity (PV) as an exact material invariant in a frictionless, stratified and rotating flow was first noticed by Rossby[1], and was defined as $((\zeta_a \cdot \nabla\theta)/\rho)$ in the dry atmosphere by Ertel[2]. The PV has three important properties: the conservation[2—4], the invertibility in a balanced system[5] and the impermeability of PV substance[3,4]. These properties are fundamental to our understanding of atmospheric dynamics and thermodynamics[6].

In moist atmosphere, the potential temperature is replaced by the equivalent potential temperature in the definition of PV, which is referred to as the moist potential vorticity (MPV). MPV has similar properties to PV[7,8]. PV/MPV, whose variations represent synthetically the dynamic and thermodynamic changes of atmosphere, has been a very important tool in the diagnoses of atmosphere[7,9—18].

While there are some limitations associated with the nature of PV/MPV in some kinds of practical applications. Gao et al.[19] found that the MPV cannot be applied to the analysis of the two-dimensional (2D) equatorial dynamics and thermodynamics. Here another limitation is addressed. A Meiyu front is observed in the Jiang-Huai valley of China every summer. The cyclones propagate along the steady front producing heavy rainfalls. In the vicinity of the front, the significant slopes of moist isentropic surface (equiscalar surface of equivalent potential temperature) set favorable environmental conditions for the genesis and development of cyclones[7,16—18,20]. Large MPVs occur in association with large vertical gradients of equivalent potential temperature in the upper and lower troposphere and large cyclonic vertical vorticities developing near the front, whereas relatively large horizontal gradients of equivalent potential temperature appear in mid-troposphere with relatively small vertical ones. And the vertical ones even become zero when the moist isentropic surface becomes upright (moist neutral stratification as addressed in Ref.[20]). Since the horizontal component of MPV is much less than the vertical counterpart[1)], little MPV changes are observed, which may make the analysis a little difficult.

Gao et al.[19] realized that the MPV vanishes as a 2D flow approaching to the equator, which indicates that the MPV cannot be applied to the analysis of the 2D dynamics and thermodynamics in tropics. To

* Supported by National Natural Science Foundation of China (Grant Nos. 40505012 and 40433007) and "Outstanding Overseas Scholars" Project (No.2005-2-17)

** To whom correspondence should be addressed. E-mail: xpcui@mail.iap.ac.cn

1) Gao S., Li X., Tao W. K. et al. Convective and moist vorticity vectors associated with tropical oceanic convection: A three-dimensional cloud-resolving model simulation. J. Geophys. Res., 2006, accepted.

solve the problem, a convective vorticity vector $\left(\mathrm{CVV} = \frac{\boldsymbol{\zeta}_a \times \nabla\theta_e}{\rho}\right)$ is defined as the vector product of absolute vorticity vectors and equivalent potential temperature gradients. They showed that the vertical component of the CVV is closely related to 2D tropical convections. They also studied the CVV and moist vorticity vector(MVV)[21] by using three-dimensional (3D) cloud-resolving simulation data in the tropical region[1)], which confirmed their results of 2D study. The analysis shows that the linear correlation coefficients between cloud hydrometeors and vertical components of convective and moist vorticity vectors are not only significantly larger than those between cloud hydrometeors and corresponding horizontal components, but also larger than that between cloud hydrometeors and the MPV in tropics.

In this study, the CVV and its tendency have been analyzed based on a simulation of mesoscale rainstorms in the Jiang-Huai valley of China with PSU/NCAR MM5 briefly. The questions to be answered are: What does the CVV look like in subtropical region? What is the relation between mesoscale rainstorms in the Jiang-Huai valley of China and the vertical component of the CVV? That is, is the CVV, especially its vertical component, useful for the analysis of development and movement of mesoscale rainstorms in the vicinity of the Meiyu front? We first define a 3D CVV, and then discuss the physical meaning and distributions of the new vector by a simulation of mesoscale rainstorms in the Jiang-Huai valley of China with PSU/NCAR MM5. In Section 2, the tendency equations of the CVV are derived, and the physical meaning of the equations is discussed. The summary is given in Section 3.

1 Convective vorticity vector (CVV)

As defined by Gao et al.[19], the CVV is

$$\boldsymbol{P}_c = \frac{\boldsymbol{\zeta}_a \times \nabla\theta_e}{\rho} \tag{1}$$

where $\boldsymbol{\zeta}_a = \nabla \times \boldsymbol{V} + 2\boldsymbol{\Omega}$ is the atmospheric absolute vorticity vector, ρ the moist air density and θ_e the equivalent potential temperature. The CVV can be expanded as

$$\boldsymbol{P}_c = \frac{1}{\rho}[(\zeta_2 + \tilde{f})\theta_{ez} - (\zeta_3 + f)\theta_{ey}]\boldsymbol{i} + \frac{1}{\rho}[(\zeta_3 + f)\theta_{ex} - \zeta_1\theta_{ez}]\boldsymbol{j} + \frac{1}{\rho}[\zeta_1\theta_{ey} - (\zeta_2 + \tilde{f})\theta_{ex}]\boldsymbol{k} \tag{2}$$

where $\zeta_1 = \frac{\partial w}{\partial y} - \frac{\partial v}{\partial z}$, $\zeta_2 = \frac{\partial u}{\partial z} - \frac{\partial w}{\partial x}$ and $\zeta_3 = \frac{\partial v}{\partial x} - \frac{\partial u}{\partial y}$, $f = 2\Omega\sin\varphi$ and $\tilde{f} = 2\Omega\cos\varphi$; $\nabla\theta_e = \frac{\partial\theta_e}{\partial x}\boldsymbol{i} + \frac{\partial\theta_e}{\partial y}\boldsymbol{j} + \frac{\partial\theta_e}{\partial z}\boldsymbol{k} = \theta_{ex}\boldsymbol{i} + \theta_{ey}\boldsymbol{j} + \theta_{ez}\boldsymbol{k}$.

From (2), the three components of the CVV can be written as

$$P_{c1} = \frac{1}{\rho}[(\zeta_2 + \tilde{f})\theta_{ez} - (\zeta_3 + f)\theta_{ey}] \tag{3a}$$

$$P_{c2} = \frac{1}{\rho}[(\zeta_3 + f)\theta_{ex} - \zeta_1\theta_{ez}] \tag{3b}$$

$$P_{c3} = \frac{1}{\rho}[\zeta_1\theta_{ey} - (\zeta_2 + \tilde{f})\theta_{ex}] \tag{3c}$$

To further illustrate the physical meaning of the CVV and to answer the questions proposed above, a 60-h simulation data of mesoscale rainstorms in the Jiang-Huai valley of China during 22nd—24th June 1999 with PSU/NCAR MM5 is used here. The nested-grid ratio is 1 to 3, with a fine-mesh length of 25 km and a coarse-mesh length of 75 km. The (x, y, δ) dimensions of the coarse and fine meshes are $70\times61\times23$ and $130\times106\times23$ respectively, and they are overlaid on a LAMBERT map projection true at 30°N and 60° N. The 24 δ-levels are 0.0, 0.05, 0.1, 0.15, 0.2, 0.25, 0.3, 0.35, 0.4, 0.45, 0.5, 0.55, 0.6, 0.65, 0.7, 0.75, 0.8, 0.85, 0.89, 0.93, 0.96, 0.98, 0.99, 1.0. And the pressure at the top of the model atmosphere is 70 hPa. The model is initialized at 0 GMT 22nd June 1999 with data from the NCEP 2.5° latitude-longitude global re-analysis and rawinsonde observations.

By comparing to the observations, the model reproduces well the development and movement of the rainstorms and the distribution and orientation of the torrential rain belts in the vicinity of the Meiyu Front, and reproduces well the circulations, the evolution of the Front and so on[18,22]. Fig.1 shows the observational and simulated accumulated rainfalls. The main rainfalls from 22nd to 23rd lie in Southwest China, the Jiang-Huai valley of China and the Korean peninsula in the southwest-northeast direction (Fig.1 (a), (c), (e)). The model simulates well the distribution and orientation of the rain belts in the Jiang-Huai valley of China and the Korean peninsula, while it does not give as good simulation for the rainfalls

1) See footnote 1) on page 559.

in Southwest China (Fig.1(b), (d), (f)). This may be due to the complex topography in Southwest China, which cannot be very well recognized by the model. Anyway, according to Refs.[18,22], the simulation of the rainstorms in the Jiang-Huai valley of China is good enough and the simulation data could be used for further analysis (the detailed model features, model setup and simulation verifications can be found in Refs.[18, 22]). The 3 h-interval coarse domain output is used in the current study.

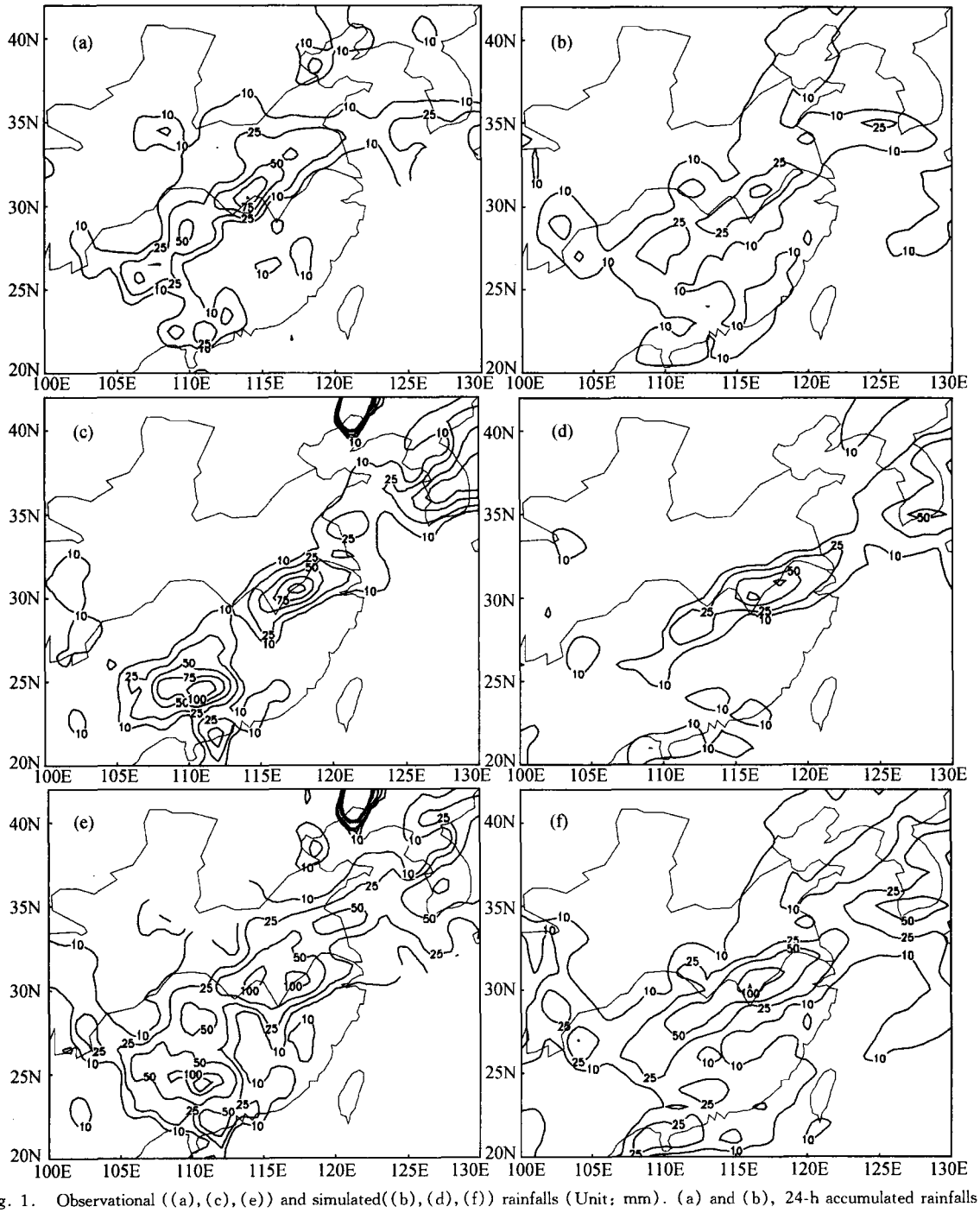

Fig. 1. Observational ((a), (c), (e)) and simulated((b), (d), (f)) rainfalls (Unit: mm). (a) and (b), 24-h accumulated rainfalls of June 22nd, 1999 (contours: 10, 25, 50, 75, 100 mm); (c) and (d), 24-h accumulated rainfalls of June 23rd, 1999(contours: 10, 25, 50, 75, 100 mm); (e) and (f), 48-h accumulated rainfalls from 22nd to 23rd June, 1999 (contours: 10, 25, 50, 100, 125 mm).

By a primary analysis with the mesoscale simulation data and according to our own results[1)], Eq.(3) could be rewritten as

$$P_{c1'} = \frac{1}{\rho}\frac{\partial u}{\partial z}\theta_{ex} \tag{4a}$$

$$P_{c2'} = \frac{1}{\rho}\frac{\partial v}{\partial z}\theta_{ex} \tag{4b}$$

$$P_{c3'} = -\frac{1}{\rho}\left[\frac{\partial v}{\partial z}\theta_{ey} + \frac{\partial u}{\partial z}\theta_{ex}\right] \tag{4c}$$

where the second part of P_{c1} and the first part of P_{c2} and the horizontal gradients of vertical velocity in Eq.(3) are relatively small and omitted from the equations. From Eq.(4) we can know that P_{c1}/P_{c2} are closely related to interactions between zonal/meridional vertical secondary circulations and convective stabilities respectively, and P_{c3} is closely related to interactions between vertical secondary circulations and horizontal equivalent potential temperature gradients. Since Gao et al. found that the vertical component of the CVV is closely related with clouds[2)], hereafter only the vertical component will be analyzed. And the horizontal components of the CVV will be discussed in other studies.

Eq.(4c) can be further divided into two parts, $P_{c31} = -\frac{1}{\rho}\frac{\partial v}{\partial z}\theta_{ey}$ and $P_{c32} = -\frac{1}{\rho}\frac{\partial u}{\partial z}\theta_{ex}$, and each part shows the interaction between the vertical (zonal or meridional) secondary circulation and the corresponding equivalent potential temperature gradient lying in the same 2D plane. Since the secondary circulations are directly associated with the vertical motion which is a direct cloud producer, and the horizontal gradients of equivalent potential temperature represent the horizontal baroclinity, the thermodynamic aspect related to convections[3)], Eq.(4c) actually can be used to study interactions between the dynamics and thermodynamics of the mesoscale rainstorms. Since the mesoscale rainstorms in the vicinity of the Jiang-Huai valley of China are always closely associated with large horizontal equivalent potential temperature gradients (the Meiyu front zone), and the stronger the rainstorms are, the more violent the interaction between the rainstorms and the front will be[18,22], P_{c3} will get robust with the development of the rainstorms and should be a good indicator for the development and movement of the mesoscale systems.

Fig.2 shows the distributions of the simulated vertical component of the CVV (vertically averaged between 850 hPa and 500 hPa) at 45 h and 51 h into the integration. P_{c3} is closely related to the development and movement of the mesoscale rainstorms and the relevant cloud systems. The distributions of P_{c3} match the variations of rainstorm-related vertical motions (Fig.2(c), (d)) and sums of cloud water and rain water (whose variations represent the development of clouds)(Fig.2(a), (b)) very well. Since P_{c3} represents the covariance between vertical secondary circulations and horizontal gradients of equivalent potential temperature, and since vertical secondary circulations are closely associated with the vertical motion which is a direct cloud and weather system producer and horizontal equivalent potential temperature gradients are directly associated with the thermodynamics related to the mesoscale systems and clouds, the good relations between the vertical components of the CVV and the development and movement of the mesoscale rainstorms are easy to be understood. According to Eq.(4c), P_{c3} has two parts, P_{c31} and P_{c32}. Fig.3 shows the distributions of the two separate parts of P_{c3} at 45 h and 51 h into the integration. It is obvious that both are closely related to the covariance between vertical wind shears (Fig.3(c)—(f)) and horizontal baroclinity (Fig.3(a), (b)), which can also be recognized from Eq.(4c). Along the Meiyu front, there are apparent horizontal equivalent potential temperature gradients (Fig.3(a), (b)), and vertical vorticities are apt to develop near the front[18], while P_{c3} is not always distinct along the front (Fig.3(a), (b)). Significant variations of the vertical component of the CVV and its two parts are mainly observed in the vicinity of the mesoscale distortions (Fig.3(a), (b)) related to the development of the rainstorms in the field of equivalent potential temperature. There are apparent couplings between strong horizontal (zonal and meridional) baroclinity (horizontal gradients of equivalent potential temperature, Fig.3(a), (b)) and vertical secondary circulations (vertical wind shears, Fig.3(c)—(f)) near the mesoscale distortions, which mainly contribute to the distinct variations of the vertical component of the CVV, P_{c3}, nearby. Actually the mesoscale distortions in the field of equivalent poten-

1) See footnote 1) on page 559.
2) See footnote 1) on page 559.
3) See footnote 1) on page 559.

tial temperature (Fig. 3(a), (b)) and other fields (figures omitted) show the apparent interactions between the rainstorms and the Meiyu Front[18,22], so the robust vertical components of the CVV near the distortions which represent exactly the interactions and covariance between dynamics and thermodynamics is standing to reason.

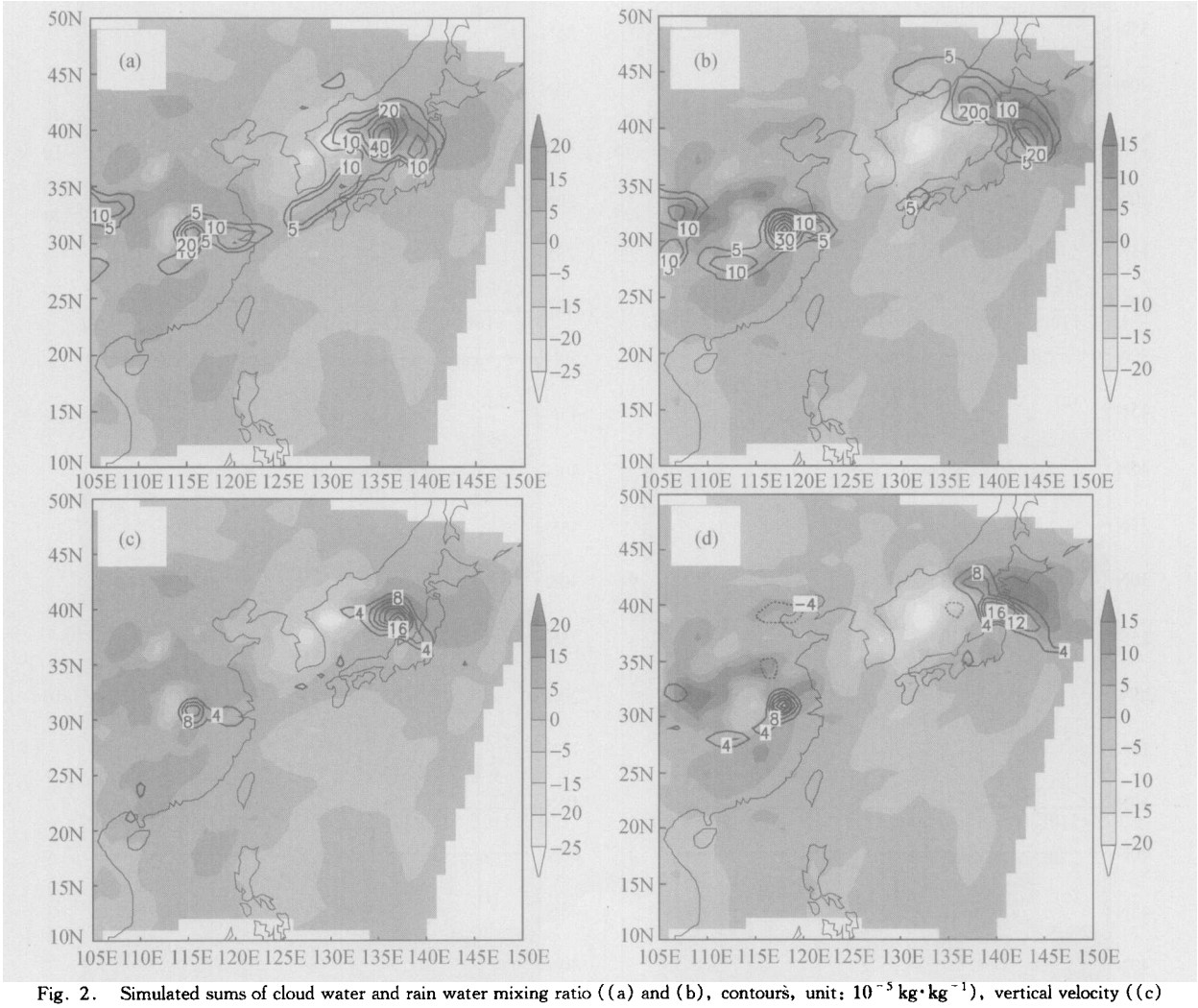

Fig. 2. Simulated sums of cloud water and rain water mixing ratio ((a) and (b), contours, unit: 10^{-5} kg·kg^{-1}), vertical velocity ((c) and (d), contours, unit: cm) and vertical components of the CVV (shadings, unit: 10^{-8} m^{2}K·kg^{-1}s^{-1}) at 45 h ((a) and (c)), and 51 h((b) and (d)) into the integration, respectively (vertically averaged between 850 hPa and 500 hPa).

2 CVV tendency equation

To further explore the physical processes responsible for the variations of the CVV, the tendency equations of the CVV are derived.

From the derivations in the appendix, the tendency equations of the three components of the CVV are

$$\frac{dP_{c1}}{dt} = CP_{11} + CP_{12} + CP_{13} + CP_{14} \quad (5a)$$

$$\frac{dP_{c2}}{dt} = CP_{21} + CP_{22} + CP_{23} + CP_{24} \quad (5b)$$

$$\frac{dP_{c3}}{dt} = CP_{31} + CP_{32} + CP_{33} + CP_{34} \quad (5c)$$

For brevity, here only (5c) will be selected to illustrate briefly the physical meaning of the tendency equation of the vertical component of the CVV.

The first term on the right-hand side of (5c) (CP_{31}) depicts the impact of the individual variation of moist air mass density caused by mass forcing from moisture phase changes[17,18] and divergence on the CVV. For example, when the CVV component P_{c3} is positive at the former moment, the mass sink of moist air (caused by heavy rains), $Q_v > 0$ (referring

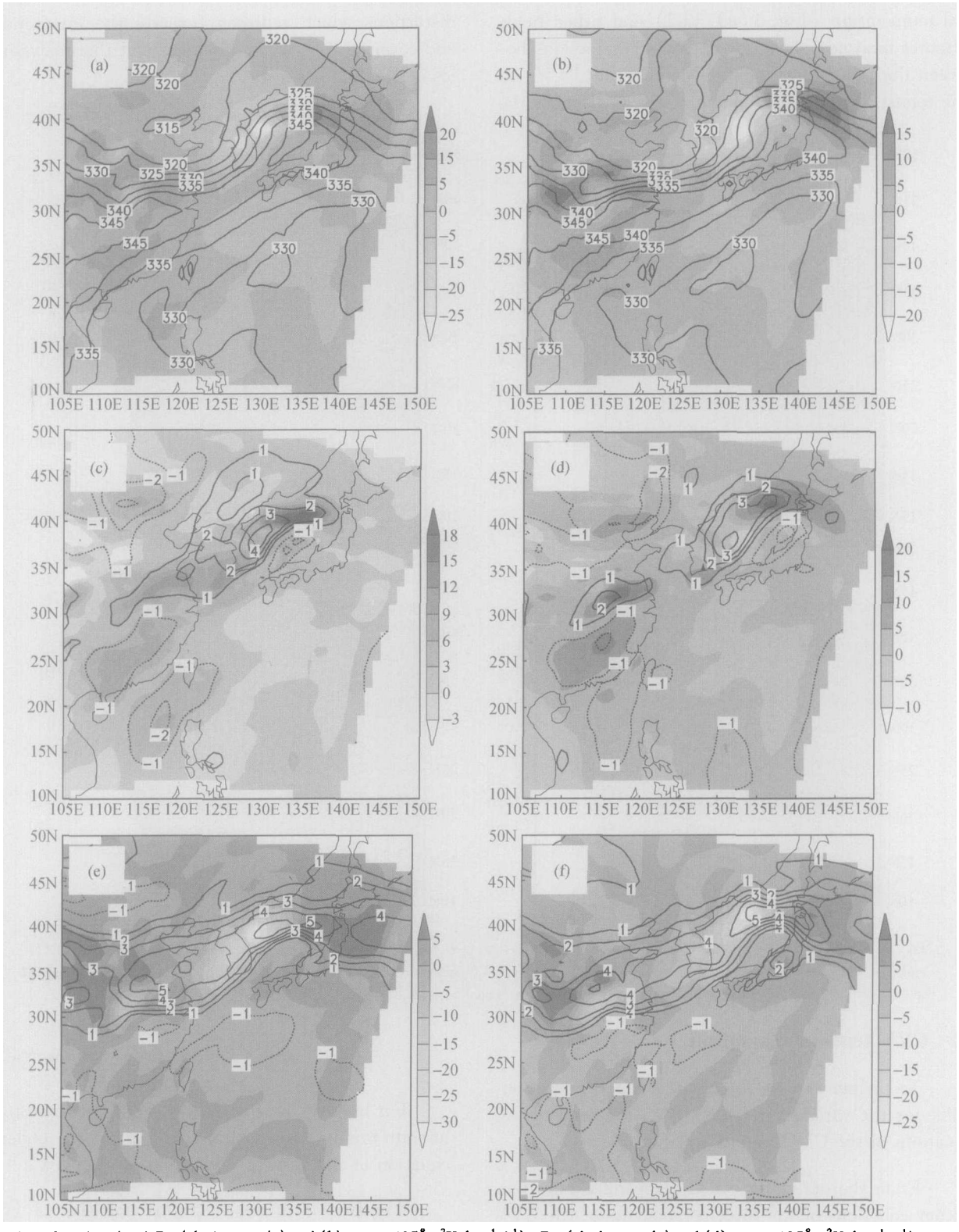

Fig. 3. Simulated P_{c3} (shadings in (a) and (b), unit: $10^{-8}\ m^2K\cdot kg^{-1}s^{-1}$), P_{c31} (shadings in (c) and (d), unit: $10^{-8}\ m^2K\cdot kg^{-1}s^{-1}$), P_{c32} (shadings in (e) and (f), unit: $10^{-8}\ m^2K\cdot kg^{-1}s^{-1}$), equivalent potential temperature (contours in (a) and (b), unit: K), vertical shears of meridional wind (contours in (c) and (d), unit: $10^{-3}\ s^{-1}$) and vertical shears of zonal wind (contours in (e) and (f), unit: $10^{-3}\ s^{-1}$) at 45 h ((a), (c) and (e)), and 51 h ((b), (d) and (f)) into the integration, respectively (vertically averaged between 850 hPa and 500 hPa).

to the appendix), will lead to positive variations of the vertical component of the CVV since moist air mass density is always positive, and vice versa. The second term (CP_{32}) depicts the influence of the interaction between atmospheric horizontal equivalent potential temperature gradients (horizontal baroclinity) and individual variations of atmospheric horizontal vorticity components (vertical secondary circulations or vertical wind shears are the main contributors to the horizontal vorticity components and the horizontal shears of the vertical wind are relatively small and omitted) on the CVV. In the vicinity of the Meiyu Front where $\theta_{ey} < 0$, if the horizontal vorticity component ζ_1 has positive (negative) individual variations, that is, the meridional vertical secondary circulation $\frac{\partial v}{\partial z}$ has negative (positive) individual variations, P_{c3} will decrease (increase) accordingly. Since the vertical secondary circulations are closely related to the vertical motions of the rainstorms, P_{c3} will evolve with the vertical motions of the rainstorms, that is, the development of the rainstorms near the slantwise isentropic surface. The third term, CP_{33}, depicts the impact of the interaction between horizontal vorticity components and individual variations of baroclinity caused by the horizontal distribution of atmospheric heating and the advection of equivalent potential temperatures by the shear of 3D wind vector on the CVV. That is, the covariance between vertical secondary circulations and the varying horizontal baroclinity or the frontogenesis/frontolysis of the Meiyu Front nearby will leads to the variation of P_{c3}. The last term, CP_{34}, represents the influence of the combination of β effect and the zonal equivalent potential temperature gradients on the CVV. In fact, this term has same physical meaning as the second term, which describes the contribution of the interaction between the individual variation of atmospheric horizontal vorticities (vertical secondary circulation, the dynamic aspect related to the development of the rainstorms) and horizontal gradients of equivalent potential temperature (the thermodynamic aspect related to the development of the rainstorms). Actually the individual variation of the vertical component of the CVV depicts the interaction between dynamic and thermodynamic aspect related to the development of the rainstorms in the vicinity of the Meiyu Front, so P_{c3} and its tendency equation could be used to trace the development and movement of the rainstorms in the Jiang-Huai valley of China.

Here only the tendency equation for the vertical component of the CVV (5c) is chosen to study the physical meaning of the CVV tendency equations and the corresponding responsible physical processes for the variation of the vertical component briefly. While even only from the simple discussion about their meaning, we can also come to a conclusion that the CVV may be a very useful tool for the study on the interaction between the vortex itself and its thermodynamic environments or the interaction between dynamics and thermodynamics of the rainstorms and trace the development and movement of the rainstorms themselves. More detailed discussions on the physical meaning of the CVV and its tendency equations will be addressed later.

3 Summary

The three-dimensional expression for convective vorticity vector, $\boldsymbol{P}_c = P_{c1}\boldsymbol{i} + P_{c2}\boldsymbol{j} + P_{c3}\boldsymbol{k}$, is provided in this paper by the vector product of atmospheric absolute vorticity vector and the gradient of equivalent potential temperature, and the brief discussion on the physical meaning of the CVV shows that the CVV depicts the interaction between atmospheric vorticity and relevant thermodynamic conditions (baroclinity and stability) or the interactions between atmospheric motions and atmospheric heating distribution, which, in tropics, depicts the interaction between vorticities and convective heating[19]1). Based on a simulation of mesoscale rainstorms in the Jiang-Huai valley of China, the vertical component of the CVV, P_{c3}, and its variations are analyzed. The distributions of P_{c3} match the variations of vertical motions and the hydrometeors very well. According to Eq. (4c), Along the Meiyu Front, especially near the mesoscale distortions in the field of equivalent potential temperatures (caused by the interactions between dynamics and thermodynamics of the mesoscale rainstorms), there are apparent couplings between strong horizontal baroclinity and vertical secondary circulations, which mainly contribute to the variations of the vertical component of the CVV. From the precise atmospheric dynamic and thermodynamic equations, the tendency equations of the three components of the CVV are derived with friction, diabatic heating and source/sink effects of moisture caused by phase changes, and the simple discussion about the physical meaning of

1) See footnote 1) on page 559.

the equations with the third equation (5c) as an example tells that the individual variation of the CVV is closely related with the individual variation of moist air mass density (by divergences and source/sink effects of moisture), interactions between the individual changes of horizontal vorticities (vertical secondary circulations) and horizontal baroclinity (horizontal gradients of equivalent potential temperature), interactions between the individual changes of horizontal baroclinity and horizontal vorticity components and β effect.

This paper gives a brief inspection to the CVV, its tendency equations and its possible application in the study of mesoscale rainstorms in the Jiang-Huai valley of China. In future work, the physical meaning of the CVV and its tendency equations will be readdressed in a more detailed context and will be applied to more case studies of mesoscale rainstorms.

Appendix

The derivation of the tendency equations of the CVV

In the local Cartesian coordinates in a tangent-plane representation, the atmospheric momentum equations can be expressed by

$$\frac{du}{dt} - fv = -\frac{1}{\rho}\frac{\partial p}{\partial x} + F_x - \tilde{f}\,w \qquad \text{(A1a)}$$

$$\frac{dv}{dt} + fu = -\frac{1}{\rho}\frac{\partial p}{\partial y} + F_y \qquad \text{(A1b)}$$

$$\frac{dw}{dt} = -\frac{1}{\rho}\frac{\partial p}{\partial z} - g + F_z + \tilde{f}\,u \qquad \text{(A1c)}$$

By taking $\frac{\partial(\text{A1c})}{\partial y} - \frac{\partial(\text{A1b})}{\partial z}$, $\frac{\partial(\text{A1a})}{\partial z} - \frac{\partial(\text{A1c})}{\partial x}$ and $\frac{\partial(\text{A1b})}{\partial x} - \frac{\partial(\text{A1a})}{\partial y}$, the vorticity equations can be

$$\frac{d\zeta_1}{dt} = f\frac{\partial u}{\partial z} - \zeta_1\left(\frac{\partial v}{\partial y} + \frac{\partial w}{\partial z}\right) + \left(\frac{\partial u}{\partial z}\frac{\partial v}{\partial x} - \frac{\partial u}{\partial y}\frac{\partial w}{\partial x}\right) + \frac{1}{\rho^2}\left(\frac{\partial \rho}{\partial y}\frac{\partial p}{\partial z} - \frac{\partial \rho}{\partial z}\frac{\partial p}{\partial y}\right) + \left(\frac{\partial F_z}{\partial y} - \frac{\partial F_y}{\partial z}\right) + \left(\tilde{f}\frac{\partial u}{\partial y} + \frac{\partial \tilde{f}}{\partial y}u\right) = \xi_1 \qquad \text{(A2a)}$$

$$\frac{d\zeta_2}{dt} = f\frac{\partial v}{\partial z} - (\zeta_2 + \tilde{f})\left(\frac{\partial u}{\partial x} + \frac{\partial w}{\partial z}\right) + \left(\frac{\partial v}{\partial x}\frac{\partial w}{\partial y} - \frac{\partial v}{\partial z}\frac{\partial u}{\partial y}\right) + \frac{1}{\rho^2}\left(\frac{\partial \rho}{\partial z}\frac{\partial p}{\partial x} - \frac{\partial \rho}{\partial x}\frac{\partial p}{\partial z}\right) + \left(\frac{\partial F_x}{\partial z} - \frac{\partial F_z}{\partial x}\right) = \xi_2 \qquad \text{(A2b)}$$

$$\frac{d\zeta_3}{dt} = -\frac{\partial f}{\partial y}v - (\zeta_3 + f)\left(\frac{\partial u}{\partial x} + \frac{\partial v}{\partial y}\right) + \left(\frac{\partial w}{\partial y}\frac{\partial u}{\partial z} - \frac{\partial w}{\partial x}\frac{\partial v}{\partial z}\right) + \frac{1}{\rho^2}\left(\frac{\partial \rho}{\partial x}\frac{\partial p}{\partial y} - \frac{\partial \rho}{\partial y}\frac{\partial p}{\partial x}\right) + \left(\frac{\partial F_y}{\partial x} - \frac{\partial F_x}{\partial y}\right) + \left(\tilde{f}\frac{\partial w}{\partial y} + \frac{\partial \tilde{f}}{\partial y}w\right) = \xi_3 \qquad \text{(A2c)}$$

The thermodynamic equation can be written as

$$C_p\frac{T}{\theta}\frac{d\theta}{dt} = -L\frac{dq}{dt} + Q_d \qquad \text{(A3)}$$

By replacing potential temperature with equivalent potential temperature in (A3), we get

$$\frac{\partial \theta_e}{\partial t} = -u\frac{\partial \theta_e}{\partial x} - v\frac{\partial \theta_e}{\partial y} - w\frac{\partial \theta_e}{\partial z} + Q \qquad \text{(A4)}$$

where $Q = \frac{\theta_e}{C_pT}Q_d$. By taking $\frac{\partial}{\partial x}$, $\frac{\partial}{\partial y}$ and $\frac{\partial}{\partial z}$ (A4) we get

$$\frac{d\theta_{ex}}{dt} = -\frac{\partial u}{\partial x}\theta_{ex} - \frac{\partial v}{\partial x}\theta_{ey} - \frac{\partial w}{\partial x}\theta_{ez} + \frac{\partial Q}{\partial x} \qquad \text{(A5a)}$$

$$\frac{d\theta_{ey}}{dt} = -\frac{\partial u}{\partial y}\theta_{ex} - \frac{\partial v}{\partial y}\theta_{ey} - \frac{\partial w}{\partial y}\theta_{ez} + \frac{\partial Q}{\partial y} \qquad \text{(A5b)}$$

$$\frac{d\theta_{ez}}{dt} = -\frac{\partial u}{\partial z}\theta_{ex} - \frac{\partial v}{\partial z}\theta_{ey} - \frac{\partial w}{\partial z}\theta_{ez} + \frac{\partial Q}{\partial z} \qquad \text{(A5c)}$$

Following Ref.[8] and Refs.[17,18], the continuity equations can be expressed by

$$\frac{d\rho_d}{dt} + \rho_d\nabla\cdot\boldsymbol{V} = 0 \qquad \text{(A6a)}$$

$$\frac{d\rho_v}{dt} + \rho_v\nabla\cdot\boldsymbol{V} = -Q_v \qquad \text{(A6b)}$$

$$\frac{d\rho_w}{dt} + \rho_w\nabla\cdot\boldsymbol{V} + \nabla\cdot(\rho_r\boldsymbol{V}_t) = Q_v \qquad \text{(A6c)}$$

where ρ_d, ρ_v, ρ_c and ρ_r are the densities of dry air, vapor, cloud water and rain water, respectively; $\rho_w = \rho_c + \rho_r$; Q_v is the conversion from vapor to cloud water and rain water. Air continuity equation is obtained by the addition of (A6a) and (A6b),

$$\frac{d\rho}{dt} + \rho\nabla\cdot\boldsymbol{V} = -Q_v \qquad \text{(A7)}$$

where $\rho = \rho_d + \rho_v$ is the density of moist air.

Taking the material derivative to both sides of (3a), (3b) and (3c), we get

$$\frac{dP_{c1}}{dt} = -\frac{P_{c1}}{\rho}\frac{d\rho}{dt} + \frac{1}{\rho}\left[\theta_{ez}\frac{d\zeta_2}{dt} - \theta_{ey}\frac{d\zeta_3}{dt}\right] + \frac{1}{\rho}\left[(\zeta_2 + \tilde{f})\frac{d\theta_{ez}}{dt} - (\zeta_3 + f)\frac{d\theta_{ey}}{dt}\right]$$

$$+\frac{v(\tilde{\beta}\,\theta_{ez}-\beta\theta_{ey})}{\rho} \tag{A8a}$$

$$\frac{dP_{c2}}{dt}=-\frac{P_{c2}}{\rho}\frac{d\rho}{dt}+\frac{1}{\rho}\left[\theta_{ex}\frac{d\zeta_3}{dt}-\theta_{ez}\frac{d\zeta_1}{dt}\right]+\frac{1}{\rho}\left[(\zeta_3+f)\frac{d\theta_{ex}}{dt}-\zeta_1\frac{d\theta_{ez}}{dt}\right]+\frac{\beta v\theta_{ex}}{\rho} \tag{A8b}$$

$$\frac{dP_{c3}}{dt}=-\frac{P_{c3}}{\rho}\frac{d\rho}{dt}+\frac{1}{\rho}\left[\theta_{ey}\frac{d\zeta_1}{dt}-\theta_{ex}\frac{d\zeta_2}{dt}\right]+\frac{1}{\rho}\left[\zeta_1\frac{d\theta_{ey}}{dt}-(\zeta_2+\tilde{f})\frac{d\theta_{ex}}{dt}\right]-\frac{\tilde{\beta}\,v\theta_{ex}}{\rho} \tag{A8c}$$

where $\tilde{\beta}=\dfrac{\partial\tilde{f}}{\partial y}$.

(A8) are the tendency equations of the three components of the CVV. The first terms on the right-hand sides of the three equations represent the impacts of the density variations on the CVV. The second terms on the right-hand sides denote the contributions of the interactions between the changes of atmospheric vorticities and the equivalent potential temperature gradients to the CVV. The third terms on the right-hand sides are the contributions of the interactions between the changes of the equivalent potential temperature gradients and atmospheric vorticities to the CVV. The fourth terms on the right-hand sides are β effects.

Finally, (A8) can be expressed by

$$\frac{dP_{c1}}{dt}=CP_{11}+CP_{12}+CP_{13}+CP_{14} \tag{A9a}$$

$$\frac{dP_{c2}}{dt}=CP_{21}+CP_{22}+CP_{23}+CP_{24} \tag{A9b}$$

$$\frac{dP_{c3}}{dt}=CP_{31}+CP_{32}+CP_{33}+CP_{34} \tag{A9c}$$

where

$$CP_{11}=\frac{P_{c1}}{\rho}(\rho\nabla\cdot\boldsymbol{V}+Q_v) \tag{A10a}$$

$$CP_{12}=\frac{1}{\rho}(\theta_{ez}\xi_2-\theta_{ey}\xi_3) \tag{A10b}$$

$$CP_{13}=\frac{1}{\rho}\left[(\zeta_2+\tilde{f})\left(\frac{\partial Q}{\partial z}-\frac{\partial\boldsymbol{V}}{\partial z}\cdot\nabla\theta_e\right)-(\zeta_3+f)\left(\frac{\partial Q}{\partial y}-\frac{\partial\boldsymbol{V}}{\partial y}\cdot\nabla\theta_e\right)\right] \tag{A10c}$$

$$CP_{14}=\frac{v(\tilde{\beta}\,\theta_{ez}-\beta\theta_{ey})}{\rho} \tag{A10d}$$

$$CP_{21}=\frac{P_{c2}}{\rho}(\rho\nabla\cdot\boldsymbol{V}+Q_v) \tag{A10e}$$

$$CP_{22}=\frac{1}{\rho}(\theta_{ex}\xi_3-\theta_{ez}\xi_1) \tag{A10f}$$

$$CP_{23}=\frac{1}{\rho}\left[(\zeta_3+f)\left(\frac{\partial Q}{\partial x}-\frac{\partial\boldsymbol{V}}{\partial x}\cdot\nabla\theta_e\right)-\zeta_1\left(\frac{\partial Q}{\partial z}-\frac{\partial\boldsymbol{V}}{\partial z}\cdot\nabla\theta_e\right)\right] \tag{A10g}$$

$$CP_{24}=\frac{\beta v\theta_{ex}}{\rho} \tag{A10h}$$

$$CP_{31}=\frac{P_{c3}}{\rho}(\rho\nabla\cdot\boldsymbol{V}+Q_v) \tag{A10i}$$

$$CP_{32}=\frac{1}{\rho}(\theta_{ey}\xi_1-\theta_{ex}\xi_2) \tag{A10j}$$

$$CP_{33}=\frac{1}{\rho}\left[\zeta_1\left(\frac{\partial Q}{\partial y}-\frac{\partial\boldsymbol{V}}{\partial y}\cdot\nabla\theta_e\right)-(\zeta_2+\tilde{f})\left(\frac{\partial Q}{\partial x}-\frac{\partial\boldsymbol{V}}{\partial x}\cdot\nabla\theta_e\right)\right] \tag{A10k}$$

$$CP_{34}=-\frac{\tilde{\beta}\,v\theta_{ex}}{\rho} \tag{A10l}$$

References

1 Rossby CG. Dynamics of steady ocean currents in the light of experimental fluid mechanics. Mass. Inst. of Technology and Woods Hole Oc. Instn. Papers in Physical Oceanography and Meteorology, 1936, 5: 1—43

2 Ertel H. Ein neuer hydrodynamischer wirbelsatz. Meteorology Zeitschr Braunschweigs, 1942, 6: 277—281

3 Haynes PH and McIntyre ME. On the evolution of vorticity and potential vorticity in the presence of diabatic heating and frictional or other forces. J Atmos Sci, 1987, 44: 828—841

4 Haynes PH and McIntyre ME. On the conservation and impermeability theorems for potential vorticity. J Atmos Sci, 1990, 47: 2021—2031

5 McIntyre ME and Norton WA. Potential-vorticity inversion on a hemisphere. J Atmos Sci, 2000, 57: 1214—1235

6 Hoskins BJ, McIntyre ME and Robertson AW. On the use and significance of isentropic potential vorticity maps. Quart J R Met Soc, 1985, 111: 877—946

7 Wu G and Liu H. Vertical vorticity development owing to downsliding at slantwise isentropic surface. Dynamics of Atmospheres and Oceans, 1998, 27: 715—743

8 Gao S, Lei T and Zhou Y. Moist potential vorticity anomaly with heat and mass forcings in torrential rain systems. Chin Phys Lett, 2002, 19: 878—880

9 Bennetts DA and Hoskins BJ. Conditional symmetric instability-a possible explanation for frontal rainbands. Quart J Roy Meteor Soc, 1979, 105: 945—962

10 Emanuel KA. Inertial instability and mesoscale convective systems. Part I: Linear theory of inertial instability in rotating viscous fluids. J Atmos Sci, 1979, 36: 2425—2449

11 Danielsen EF and Hipskind RS. Stratospheric-tropospheric exchange at polar latitudes in summer. J Geophys Res, 1980, 85 (C1): 393—400

12 Thorpe AJ. Diagnosis of balanced vortex structure using potential vorticity. J Atmos Sci, 1985, 42: 397—406

13 Hoskins BJ and Berrisford P. A potential vorticity perspective of the storm of 15—16 October 1987. Weather, 1988, 43: 122—129

14 Cao Z and Cho H. Generation of moist vorticity in extratropical cyclones. J Atmos Sci, 1995, 52: 3263—3281
15 Cho H and Cao Z. Generation of moist vorticity in extratropical cyclones. Part Ⅱ: Sensitivity to moisture distribution. J Atmos Sci, 1998, 55: 595—610
16 Cui X, Wu G and Gao S. A numerical simulation and isentropic analysis of frontal cyclones over the Western Atlantic Ocean, Acta Meteor. Sin. (in Chinese), 2002, 60: 385—399
17 Cui X, Gao S and Wu G. Moist potential vorticity and up-sliding slantwise vorticity development. Chin Phys Lett, 2003a, 20: 167—169
18 Cui X, Gao S and Wu G. Up-sliding slantwise vorticity development and the complete vorticity equation with mass forcing. Advs Atmos Sci, 2003b, 20: 825—836
19 Gao S, Ping F, Li X, et al. A convective vorticity vector associated with tropical convection: A two-dimensional cloud-resolving modeling study. J Geophys Res, 2004, 109: D14106
20 Xu H and Ding Z. The neutral condition of moist vertical motion and the formation of meso-β system. Acta Meteor Sin (in Chinese), 1997, 55: 602—610
21 Gao S, Cui X, Zhu Y, et al. A modeling study of moist and dynamic vorticity vectors associated with 2D tropical convection. J Geophys Res, 2005, 110: D17104
22 Cui X. Study on slantwise vorticity development of subtropical cyclones. Ph.D thesis, Chinese Academy of Sciences, 2001, 146